

TEMPORAL AND SPATIAL PATTERNS IN THE CATCH RATIO OF ADULT YELLOWFIN FOR THE WEST INDIAN PURSE SEINE FISHERY, 1984-2014

Francis Marsac¹ and Laurent Floch²

Abstract

Time series of catch at size from the Indian Ocean European purse seine fisheries are used to investigate the trend and spatial characteristics of the ratio of adult yellowfin (YFT) in the catch during 1984-2014. The analysis is conducted on an annual basis along 30 “biological years” which are defined from July to June of the following year in order to cover a full recruitment cycle. The size at first maturity L_{50} is the threshold used to define the spawning stock, and two extreme estimates of L_{50} are tested in the study, at 76 and 112 cm, thus defining R76 and R112 ratios, respectively. The ratios are calculated by 5° grid box, representing the percentage of adults (able to spawn during the spawning season) over the YFT purse seine catch of the year. The specific size structuring of free-swimming and object-associated catches are accounted for, however the annual ratios analyzed further combine both school types. The temporal and spatial patterns are analyzed by empirical orthogonal functions (EOF), a form of component principal analysis, and only the first two axes of the analysis, that gather 54% of the variance, are discussed. At the scale of the whole fished area, we observe an overall decline of the spawners’ ratios, independently of the catch level. Two major dips are seen in the series, likely to result from different causes. The first dip developed during the intense 1997-98 El Niño which affected catches and occurrence of free-swimming schools. The second dip which happened between 2008 and 2011 is likely due to a change in fishing tactics and strategies at the climax of the Somalian piracy. The EOFs show the ratios’ decline mostly affected the fishing area harvested by the PS fleets since 1984. It also underlined two areas of strong positive anomalies in spawners’ ratio at the extreme West (African coast) and East (Southwest Maldives) sectors of the core PS fishing zone. The results suggest a significant long-term deterioration of the YFT spawning stock status. However, a detailed analysis of the abundance trend of free schools needs to be undertaken, using observers’ data or by implementing aerial surveys, in order to better understand the causes of the decline of adult ratios in the PS catch.

1. Introduction

Yellowfin (YFT) is a major tuna species caught by tropical purse seiners. In the Indian Ocean, the purse seine contributed to 39% of the YFT catch during 1984-2014, way above longline (29%) and gillnets (15%) (Fig. 1) Even during the past 5 years, the contribution by purse seine is above 35%, whereas the share of gillnets has substantially increased (23%).

¹ IRD/ICEMASA, UMR 248 MARBEC, Avenue Jean Monnet, 34203 Sete cedex, France (francis.marsac@ird.fr)

² IRD, UMR 248 MARBEC, Avenue Jean Monnet, 34203 Sete Cedex, France

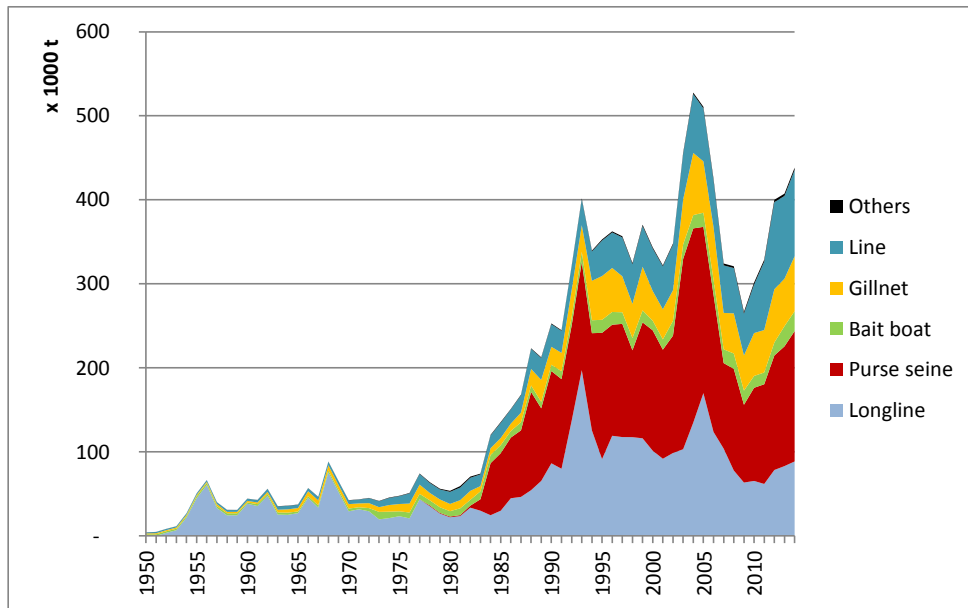
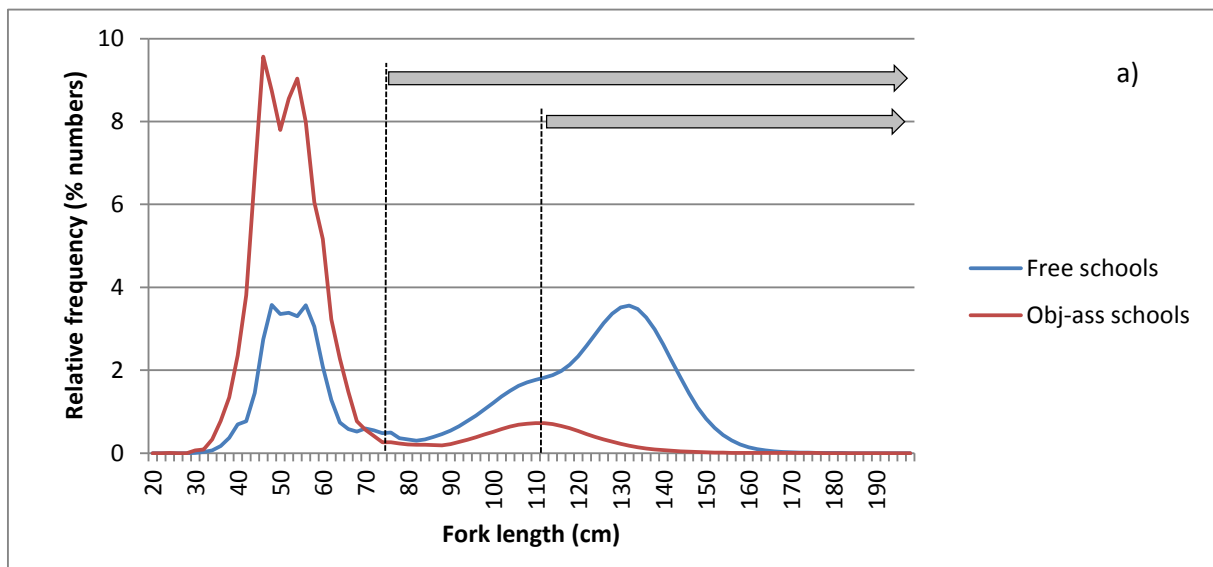


Fig. 1 : Yellowfin catches by gear, 1950-2014 (source: IOTC)

The purse seiners harvest yellowfin gathered in free-swimming schools and object-associated schools. These two fishing practices have very specific size distribution (Fig. 2). Yellowfin caught on free schools is distributed in two distinct size modes (40-65 cm and 90-170 cm) peaking at a similar frequency of individuals (3.5% in numbers). Obviously, the distribution in weight is dominated by the second mode. Object-associated catches exhibit two dissymmetrical size modes in numbers: a dominant one (40-65cm) peaking at 8 to 9.6% and a secondary mode (90-130cm) peaking at 0.7% (Fig. 2). The distribution in weight gives a more balanced distribution of the 2 modes. It is clear that the second size mode on free schools is made of more numerous and larger individuals than the second mode on object-associated schools.



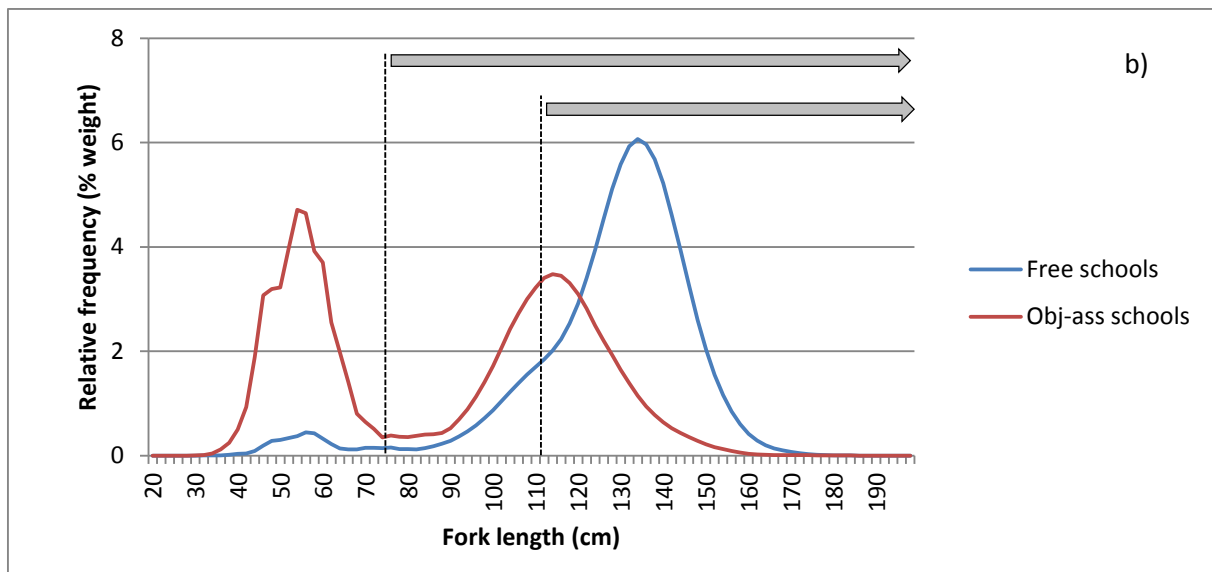


Fig. 2 – Yellowfin size distribution by fishing mode. a) in % of numbers; b) in % of weight. The dashed vertical lines denote the two size thresholds used in this study to define adult fish (i.e. above size at first maturity – see text). The two horizontal arrows denote the size range that is considered in the rest of the paper for calculating the proportion of YFT spawners in the PS catches.

The size at first maturity is a metrics used to estimate the spawning fraction of the population. Size at first maturity (L_{50}) is defined as the size where 50% of the individuals are mature. The issue is to define what characterizes a reproductive individual. The classical approach is based on macroscopic aspects of ovaries and testes at different maturation stages. Such approach applied on yellowfin in the Indian waters by Maldenya and Joseph (1985) estimated L_{50} to 104 cm. Hassani and Stéquent (1991), in the West Indian purse seine fishery, proposed L_{50} at 112 cm. The approach making use of the gonadosomatic index as a reproductive flag to estimate L_{50} (Fontoura et al, 2009) was not applied in the Indian Ocean. A third approach uses the histology to stage the females. The most recent study in this respect is that of Zudaire et al (2013) who based their L_{50} estimate on the assumption that females with ovaries at the cortical alveolar stage onward were mature (Brown-Peterson et al., 2011). This assumption provided a L_{50} value of 75 cm fork length. They also used a second estimate considering that females with advanced vitellogenic oocytes were mature, which provided a L_{50} value of 102 cm FL.

The reproductive cycle for yellowfin in the West Indian Ocean is well known. The review by Stequent and Marsac (1989) pointed out that the core spawning season was during the north-west monsoon. This was confirmed by Hassani and Stéquent (1991) using gonado somatic indices, then later by Stéquent et al (2001). The gonad maturation process starts in October and peaks in December/January. The spawning season of the West Indian Ocean yellowfin tuna is therefore defined from October to April. The core spawning zone is located in the south equatorial region, between 2°S and 10°S, where purse seiners have historically targeted free-swimming schools essentially composed of adult and mature yellowfin from December to March.

The IOTC has recommended the development of alternative methods to complement the interpretation of stock assessment model outputs. In this paper, we use the spatialized catch-at-size of the purse seine fleets operating the West Indian Ocean to analyze the temporal and spatial pattern of the mature fraction of the yellowfin population on an annual basis. This study is carried out by combining the two types of schools, free and object-associated, as they both include potential spawners.

2. Data and methods

Catch-at-size data

Although yellowfin tuna is exploited by a great variety of gears in the Indian Ocean, we selected the purse seine catch-at-size (CAS) data set established for the European fleets because of its high sampling rate ($u=93\%$, $s=7\%$) and data reliability. Indeed, size data exist for the longline contributing to 29% of the yellowfin catch, but the low (and time-varying) sampling rate of the actual catches ($u=13\%$, $s=13\%$ for all longline fleets combined) is a strong limitation for the kind of analysis performed in this paper.

The PS CAS dataset used covers the period 1984-2014. We used “biological years” starting in July of year y and ending in June of year $y+1$. This is to account for the fact that larvae batches and the unfished fraction of the population (< 30 cm) develop during the first semester, before recruitment occurs in the PS fishery at the start of the second semester. If calendar years were considered, the spawning season (and the maximum abundance of spawners) would be cut off between two consecutive years, which is not satisfactory in terms of year inter-comparison and temporal trend. Therefore, the study spans 30 years, from July 1984 to June 2014.

The size data aggregated by month, along a 5-degree grid, were raised to the PS catch of each 5°-month strata using the length-weight relationship $W = 1.886 \cdot 10^{-5} * L^{3.0195}$, with W in kg and L in cm (Marsac et al, 2006). As we only focus on inter-annual changes, we discarded the monthly/seasonal cycle by doing all further calculations on an annual basis. Then, for each biological year, we calculated the ratio (in percent) of adult fish (i.e. having the ability to mature and spawn over the year) in dividing the weight of individuals above L_{50} by the total weight of the species in the fishery.

$$R_{ij} = \frac{\sum_{L_{50}}^{L_{max}} W_{lij}}{C_j} \times 100$$

with i representing the 5° grid box, j the biological year, W_l the weight of the corresponding size interval between L_{50} and the maximum length sampled (L_{max}), and C_j the PS yellowfin catch of the year in the whole fished area. The ratios are calculated for each school type separately, then summed in each 5° grid box and year.

The resulting ratio calculated by this method represents the spawning potential of each 5° grid box by biological years.

In order to test the sensitivity of the results, we considered two values for L_{50} : i) the smallest one (75 cm, rounded to 76 cm because of the 2 cm size structure of the dataset) following Zudaire et al (2013) and ii) the largest one (112 cm) as proposed by Hassani and Stéquent (1991). We note that the second estimate by Zudaire et al (2013) and also that of Maldenya and Joseph (1985) fall within this size range. Eventually, we obtain two ratios for the same year, one for fish larger than 76 cm (R_{76}), the other for fish larger than 112 cm (R_{112}).

Empirical orthogonal function

We used empirical orthogonal functions (EOF) to analyze simultaneously the spatial and temporal variability patterns of 5° grid box ratios. EOFs, a technique derived from the principal component analysis, have been extensively used in meteorology and oceanography to analyze space and time trends in data sets (Lorenz 1956). The method represents the data as a sum of products of functions:

$$f(x, y, t) = \sum (F_i(x, y) \cdot G_i(x, y))$$

where the F_i denote the data distribution in space and the G_i give the contribution of the respective space distribution at any given time. An infinite sum of functions will reproduce the current observations but, practically, the summation is truncated after the first few terms. The contributions of the sum are arranged in such a way that the first term (= first axis) accounts for more of the variance found in the observations than any other term. The second term accounts for most of the remaining variance and so on. The Eigen values that are calculated by this method have no unit and are proportional to deviations about the mean (standardized anomalies). The product of the spatial value

(or coefficient) for the grid point (x,y) and the value at time t gives the sign of the anomaly for the triplet (x,y,t).

Before performing an EOF, data must be converted into anomalies. We first calculated the average ratio by 5° grid box over the 30 years and then subtracted the average from the actual 5°/year ratio. We end up with a space/time series of anomaly ratios which is the 3D data matrix analyzed by the EOF program (FORTRAN script).

3. Results

Overall trend

The ratios of potential spawners by 5° grid box were summed by biological year to provide an overall estimate starting in 1984. The results are presented in Fig 3 for all school types combined.

The R76 and R112 ratios depict the same temporal pattern, although R112 shows larger inter-annual variability than R76 does. The series exhibits an overall declining trend, from levels of 80-90% (60-80%) for R76 (R112) during the 1980s, to 50-70% (35-55%) from 2008 onwards. Two major dips occurred in 1997-1999 and 2008-2010. Regarding YFT PS catches, there is a steady increase from 1984 to 2001-02, followed by 4 years of historically high catches, then a steep decline in 2006-07 until 2010-11, and a 50% increase since then. At the scale of the fishery, there is no correlation between the spawners' ratios and the purse seine catches ($r^2=0.012$). For additional information (not shown in graphs), the yearly R76 on free schools mostly stands above 95% of the population exploited by the purse seine (except during a dip to 88% in 1997-1999). On object-associated schools, R76 varies in the range 30-80% with an overall declining trend from 1994-95 onwards.

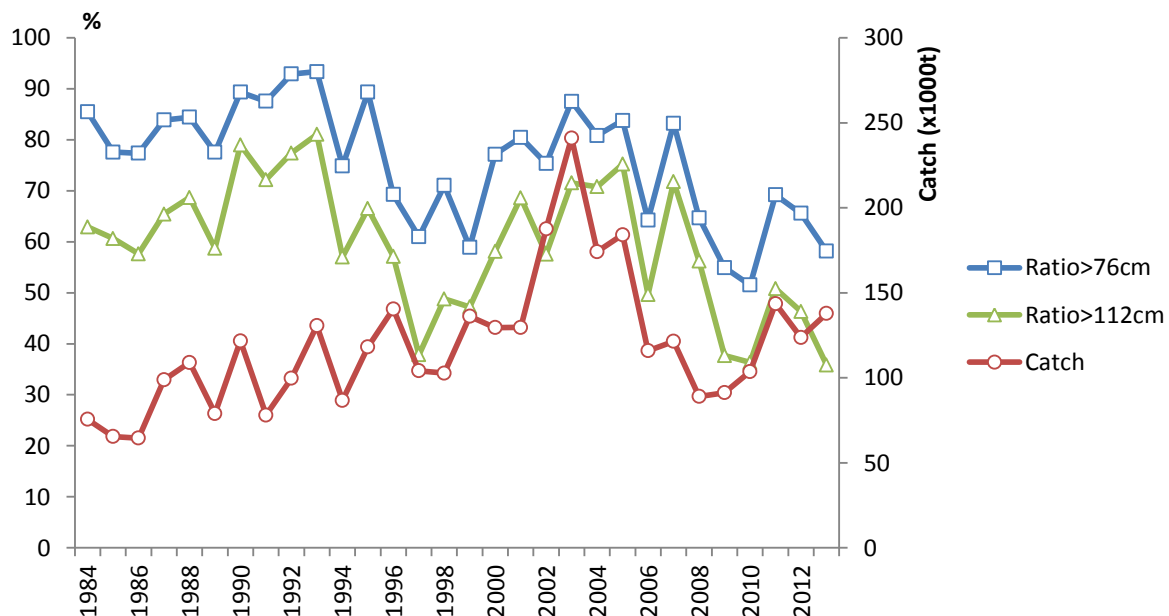


Fig. 3 – Ratio of potential YFT spawners at two size threshold (L_{50}), and corresponding purse seine catches by biological year.

Temporal and spatial patterns

We present the first 2 EOFs, which explain 54% of the total variance of the ratios. We select R76 only as both R76 and R112 EOFs have very similar patterns. The two EOFs depict distinct trends.

EOF1 (38.1%) characterizes two regimes that are depicted in the temporal component (Fig. 4a): dominant negative loadings in the early years of the PS fishery (1984-91) then large fluctuations in the positive domain from 1998 onwards, with a steep change spanning 5 years between these 2 regimes. The EOF1 spatial structure (Fig. 4b) is composed of negative values from 45° to 70°E, 0° to 10°S, and

covers most of the western core PS YFT fishing zone (bounded by the red line). West of 45°E, along the African coast, and East of 75°E (in an area with YFT catch above 1000 t/5° square), the loadings become highly positive. The corresponding R76 ratios are the product of the temporal and spatial loadings. Between 45° and 70°E, this indicates the R76 ratios explained by EOF1 have declined since the inception of the PS fishery, particularly from 60° to 65°E (e.g. for 1988, the product of negative temporal and spatial values gives a positive ratio anomaly). In the early years, the part of R76 corresponding to EOF1 was 3 to 6% above the long term annual average whereas it fell to 3 to 6% below the average during 1997-2000, 2007-2010 and 2013-14. By contrast, in areas with positive spatial loadings, R76 was relatively low in the early years of the PS fishery and became quite high between 1997-2000, 2007-2010 and 2013-14. Along the African coast, R76 depicted by EOF1 increased by 15% above the average, and up to 50% between 75° to 80°E.

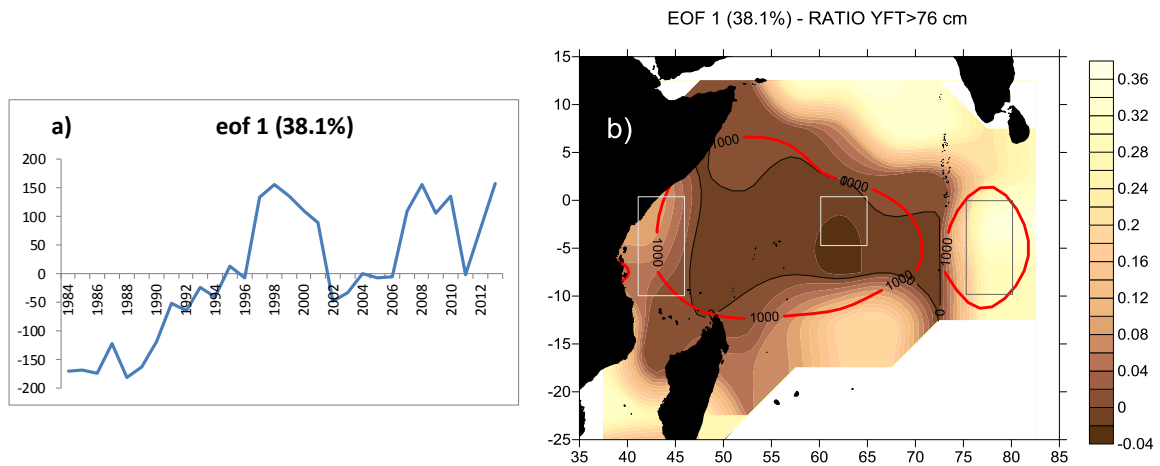


Fig. 4 – Time sequence (a) and spatial pattern (b) of the R76 ratio's first EOF. The red line bounds the areas where the YFT PS catches are above 1000 t per 5° grid box. The rectangular boxes on the map delineate three areas where R76 and R112 will be further analyzed (see Fig. 6)

EOF2 (15.7%) depicts two major anomalies (1992-1995 and 2002-2006) but no trend (Fig. 5a). Between 0°-5°S / 45°-70°E, R76 ratios explained by EOF2 did not vary much about the long term mean in 1992-1995 (as the spatial values are close to 0). By contrast, R76 was substantially above the average during 1992-1995 between 5°S-10°S / 70°-75°E and slightly below the average in 2002-2006 (Fig. 5b).

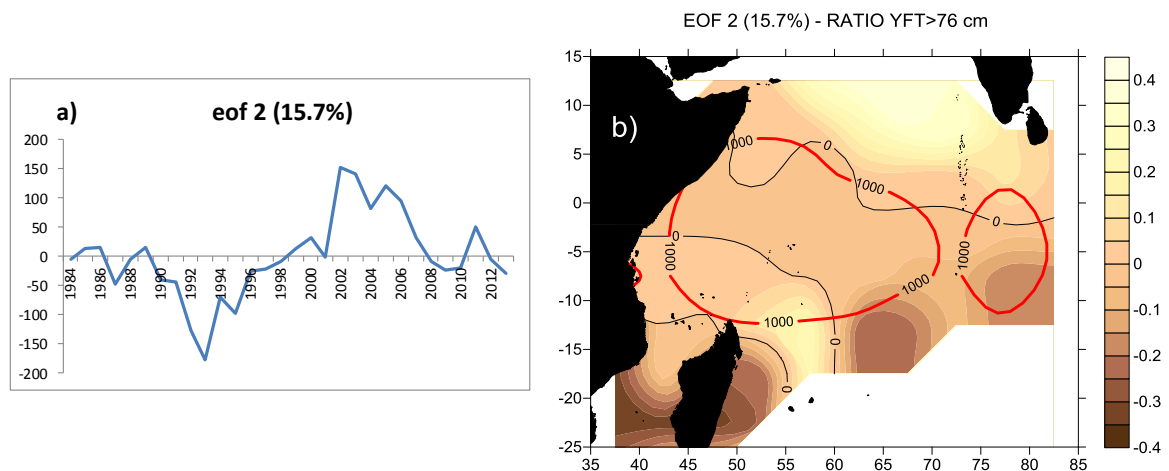


Fig. 5 – Time sequence (a) and spatial pattern (b) of the R76 ratio's second EOF. The red line bounds the areas where the YFT PS catches are above 1000 t per 5° grid box.

Case studies

Three areas located in the largest spatial anomalies depicted in Fig. 4b were selected to illustrate the R76 and R112 ratios' inter-annual variability.

Along the African coast (Fig. 6a) the most significant anomaly occurred from 2001-02 to 2004-2005. During this period, the westernmost box (which covers two 5° squares) gathered more than 40% of the mature fish of the whole area fished yearly by PS. In the core of the YFT PS fishing zone (Fig. 6b), both ratios have declined. In the 5° square selected, R76 and R72 were in 2013-14 one third of what they used to be during the first three years of the fishery. In the easternmost box, southwest of Maldives, YFT PS catches started in 1994-95, with significantly high ratios of mature fish in such a restricted area (6 and 4% during the first 2 years). Another significant anomaly occurred in 2001-02, with mature fish representing 5% of the annual PS catch.

In each of the selected areas, the ratios are highly correlated to the catch ($\alpha < 0.01$).

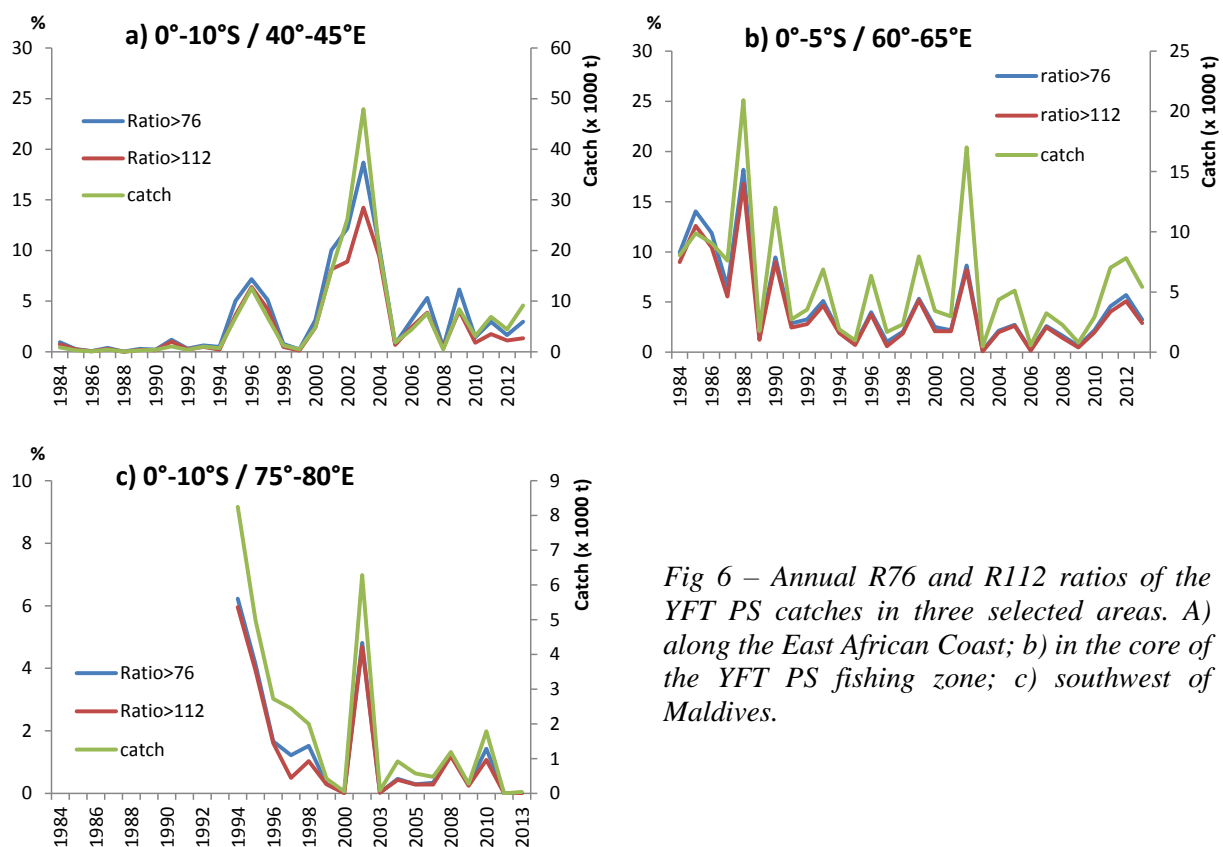


Fig 6 – Annual R76 and R112 ratios of the YFT PS catches in three selected areas. A) along the East African Coast; b) in the core of the YFT PS fishing zone; c) southwest of Maldives.

4. Discussion

The ratio of yellowfin spawners in the WIO PS fishery varies according to the school type. However, the overall trend, all school types combined, is a decline of the two ratios used in this study, R76 and R112, representing fish larger than 76 and 112 cm FL, respectively. Free schools contribute the most to the spawners' catch (annual average of 60 000 t and 52 000 t above 76 and 112 cm FL, respectively) but object-associated schools still represent a significant part of it (25 000 t and 14 000 t).

The two main dips found in the series can be attributed to different causes. The first dip developed during the intense 1997-98 El Niño, where the surface tuna schools vanished in the WIO and became probably scattered about the anomalously deep thermocline (Marsac and Le Blanc, 1999; Vialard et al,

2009). The PS free school catches were very low (33 000 t) and the decline was more severe for yellowfin of the larger sizes (>112 cm FL). The depth of the 20°C isotherm (Z20) is used as a proxy of the thermocline depth. The map of Z20 in January 1998 indicates that the thermocline was below 140 m across the core YFT PS fishing zone (Fig. 7a), representing a deep anomaly greater than 50 m (Fig. 7b). The Z20 anomaly developed in July 1997 and stretched over the whole biological year 1997-98. Other deep thermocline events of lesser magnitude happened in 1994-95 (strong positive Indian Ocean dipole event) and 2006-07 (El Niño). R112 inter-annual fluctuations are well correlated to the Z20 anomaly as shown in Fig. 7c ($R_{\text{spearman}} = -0.42$, $\alpha < 0.05$) but only if considering the period 1984-2007.

When the years 2008-2013 are added, the correlation is no longer significant ($R_{\text{spearman}} = -0.32$), indicating that an additional cause may be sought to explain the decline of spawners' ratios in the last years of the series. The PS fishery was affected by the development of the Somalian piracy in 2008 and this led to a change of fishing tactics. The number of PS in operation in the Indian Ocean decreased gradually by 30% over 2008-2011 and the effort was even more focused on object-associated schools. The consequence was a decline of free schools catches, an increase of object-associated catches and a subsequent lesser proportion of mature YFT in the catch.

Therefore, the environmental variability can be considered as the leading cause of YFT catch declines (and R72, R112 ratios) until 2007, whereas the change in fishing tactics and strategies by PS fleets due to the piracy may be seen as the leading factor of catch declines after 2008.

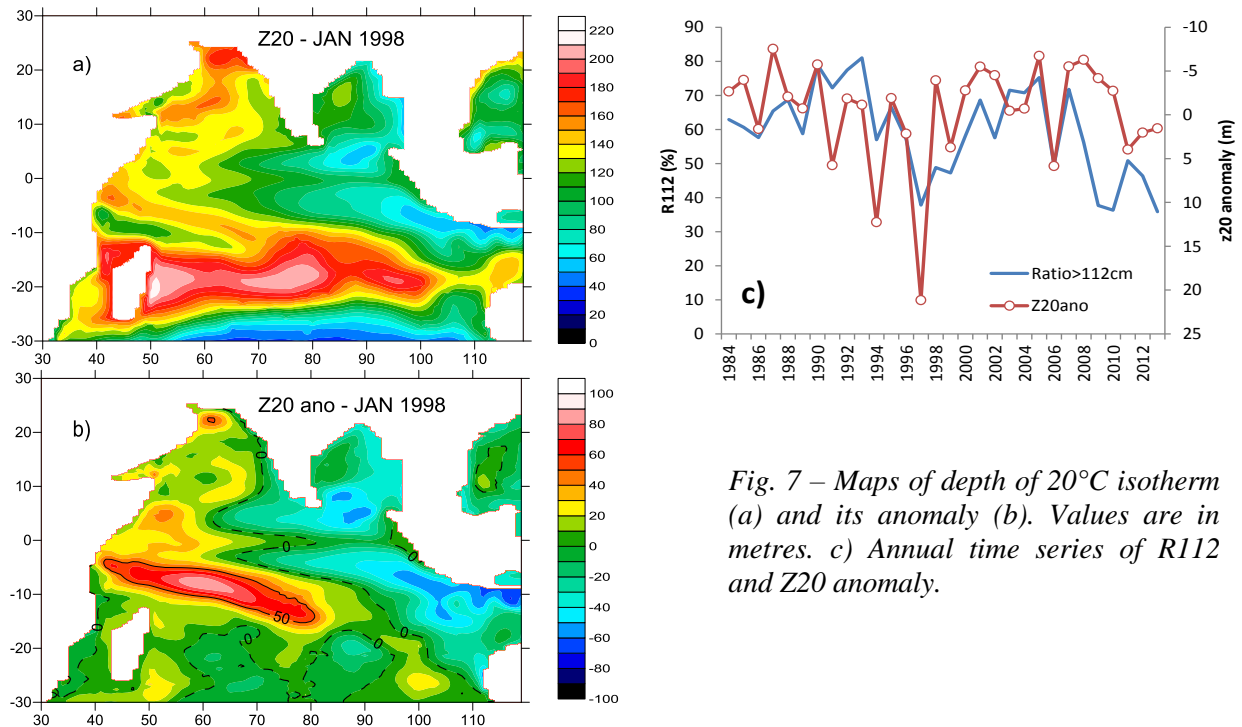


Fig. 7 – Maps of depth of 20°C isotherm (a) and its anomaly (b). Values are in metres. c) Annual time series of R112 and Z20 anomaly.

The use of EOFs provides an insight into the spatial changes of spawner's ratio. The decline of spawners' ratio was mostly seen in the fishing area harvested by the PS fleets since 1984. This trend corresponds to the first EOF: high ratios in the early years and a rapid shift to another regime dominated by ratios below the long term average. There are also two periods of strong anomalies (1992-1995 and 2002-2006) depicted by the second EOF. The two EOFs, that explain 54% of the total variance, underline strong positive anomalies in spawners' ratio at the extreme West (African coast) and East (Southwest Maldives) sectors of the core PS fishing zone.

R76 and R112 ratios are not correlated to YFT catches when we consider the whole fishing zone. By contrast, ratios and catches are well correlated in restricted areas where strong anomalies (variability) take place. This is shown in Fig 6, over the whole series. Correlations are 0.95, 0.90 and 0.98 for the western, central and eastern boxes respectively. This high degree of correlation between PS YFT catches and spawners' ratio reflects the highly concentrated nature of the schools during the spawning

season, which form dense clusters heavily exploited by purse seiners. In such situation, the spawning stock becomes well accessible and vulnerable.

The overall decline in the ratio of large individuals in the core PS fishing ground may reflect a significant deterioration of the YFT spawning stock status. Free schools which gather the bulk of spawners were a major target of PS fleets during most of the spawning season (Nov-March). YFT catches on object-associated schools, which include large individuals, have dramatically increased in the recent years. In addition, the YFT longline catches, essentially composed of large individuals, have been on a climbing trend in the recent years (35% increase from 2010 to 2014). A detailed analysis of the observer's data would be necessary to investigate whether the declining trend of large individuals can be attributed to a lesser abundance of free swimming schools, notably during the spawning season. An additional approach would be to perform line transect sampling with aerial surveys from the Seychelles.

References

- Brown-Peterson, N. J., D. M. Wyanski, F. Saborido-Rey, B. J. Macewicz, and S. K Lowerre-Barbieri (2011). A standardized terminology for describing reproductive development in fishes. *Mar. Coast. Fish.* 3:52–70.
- Fontoura, N.F., Braun, A.S., Cesar, P. and Nilani, C. (2009). Estimating size at first maturity (L50) from gonadosomatic index (GSI) data. *Neotropical Ichthyology*, 7 (2): 217-222.
- Hassani S. and B. Stequert (1991). Sexual maturity, spawning and fecundity of the yellowfin tuna (*Thunnus albacares*) of the Western Indian Ocean. *Coll. Vol. of Working Docs, IPTP*, Vol. 4, TWS/90/68: 91-107.
- Lorenz, E. 1956. Empirical orthogonal functions and statistical weather predictions. Rep. N° 1, Statistical Forecasting Programme, MIT: 49 p
- Maldenya R. and L. Joseph (1985) On the Distribution and biology of yellowfin tuna (*T. albacares*) from the Western and Southern coastal waters of Sri Lanka. *Coll. Vol. Work. Doc, IPTP*, TWS/85/21 : 51-61.
- Marsac F., M. Potier, C. Peignon, V. Lucas, P. Dewals, A. Fonteneau, R. Pianet & F. Ménard (2006). Updated biological parameters for Indian Ocean yellowfin tuna and monitoring of forage fauna of the pelagic ecosystem, based on a routine sampling at the cannery in Seychelles. *IOTC Proceedings* 9
- Marsac, F. & J-L le Blanc (1999). Oceanographic changes during the 1997-1998 El Niño in the Indian ocean and their impact on the purse seine fishery. 1st session of the IOTC working party on tropical tunas, Mahe, Seychelles, 4-8/09/99. WPTT/99/03. *IOTC Proceedings* 2 : 147-157.
- Stéquert B., J. Nuñez Rodriguez, B. Cuisset, and F. Le Menn (2001). Gonadosomatic index and seasonal variations of plasma sex steroids in skipjack tuna (*Katsuwonus pelamis*) and yellowfin tuna (*Thunnus albacares*) from the western Indian ocean. *Aquat. Living Resour.*14: 313–318.
- Stéquert, B. and F. Marsac (1989). Tropical tuna–surface fisheries in the Indian Ocean. *FAO Fish. Tech. Pap.* 282, 238 p. FAO, Rome.
- Vialard, J., J.P Duvel, M. McPhaden, P. Bouruet-Aubertot, B. Ward, E. Key, D. Bourras, R. Weller, P. Minnett, A. Weill, C. Cassou, L. Eymard, T. Fristedt, C. Basdevant, Y. Dandonneau, O. Duteil, T. Izumo, C. De Boyer Mentegut, S. Masson, F. Marsac, C. Menkes and S. Kennan (2009). Air-sea interactions in the Seychelles-Chagos thermocline ridge region. *Bulletin of the American Meteorological Society*, 90(1): 45-61
- Zudaire, I., H. Murua, M. Grande and N. Bodin (2013). Reproductive potential of yellowfin tuna (*Thunnus albacares*) in the western Indian Ocean. *Fish. Bull.* 111:252–264